June 28, 2006

Diatom vertical migration to acquire iron

Kenneth S. Johnson,[1] Zbigniew S. Kolber,[1] Joseph A. Needoba,[1] Virginia A. Elrod,[1] Steve E. Fitzwater,[1] Rachel A. Foster,[2] Denis Klimov,[1] and Sara J. Tanner[3]

[1] Monterey Bay Aquarium Research Institute, Moss Landing, California, USA.

[2] Ocean Sciences Department, University of California, Santa Cruz, California, USA.

[3] Moss Landing Marine Laboratories, Moss Landing, California, USA.

Abstract

The vertical profiles of nitrate and iron concentrations in the open ocean are characterized by sharp increases (nitracline and ferricline) beneath the sunlit euphotic zone. However, the ferricline in the Pacific Ocean is often displaced 10's to more than 100 meters below the nitracline, presenting a barrier to iron acquisition. We have observed physiological indicators of photosynthetic status in rising and sinking phytoplankton that are consistent with phytoplankton vertical migration through this displacement barrier in order to acquire iron. In addition, the nitrate above the ferricline represents a nutrient stock that could potentially contribute to a stronger biological pump that lowers atmospheric CO_2 during glacial periods with higher iron inputs.

1. Introduction

Surface ocean iron concentrations are insufficient to sustain high phytoplankton growth rates in some 40% of the ocean area [*Moore et al.*, 2004]. Open ocean iron fertilization experiments have demonstrated unambiguously that addition of iron to these systems results in increased phytoplankton growth rates and biomass accumulation [*Coale et al., 2004*]. Given the linkage between iron and biomass accumulation, pathways for iron transport into the upper ocean must be understood to assess the processes that regulate marine ecosystems and climate. Aerosol fluxes dominate inputs in most regions [*Fung et al.*, 2000; *Archer et al.*, 2000], but they are highly episodic and most flux occurs during a few months of the year [*Duce and Tindale*, 1991]. Time series observations of dissolved iron at the sea surface indicate that the dissolved iron residence time is much less than one year and the aerosol iron does not remain in the system [*Johnson et al.*, 2003; *Boyle et al.*, 2005]. Therefore, upward transport of iron becomes an important iron source during much of the year with low aerosol inputs.

A distinctive feature of vertical iron distributions at most locations in the Pacific Ocean is the presence of a ferricline at depths below the nitracline (Fig. 1). The vertical separation of the ferricline from the nitracline is found in all of the High Nitrate, Low Chlorophyll (HNLC) regions of the ocean because surface iron is depleted, but nitrate is not. It is also a common feature in much of the North and South Pacific Ocean gyres [*Johnson et al.*, 1997b], except near Hawaii where the fraction of iron that dissolves from aerosol is high [*Johnson et al.*, 2003; *Boyle et al.*, 2005].

The separation between the nitracline and ferricline is absent from any of the three-dimensional, biogeochemical models that we have examined. Although this separation

was observed at four different locations (Fig. 1), the predicted iron and nitrate profiles at these locations provided for the Los Alamos/UMaine (F. Chai, pers. comm.), Princeton (J. Dunne and J. Sarmiento, pers. comm.), MIT (M. Follows, pers. comm.), UC Irvine (J. K. Moore, pers. comm.), and NASA/Goddard (W. Gregg, pers. comm.) models place the ferricline at or above the nitracline, rather than below. This implies that the separation does not result from physical processes such as subduction of high nitrate, low iron waters at high latitude and then lateral transport of this chemical signature into the thermocline of the central gyres. Instead, it must result from biological processes not included in models.

Large diatoms, such as *Ethmodiscus rex* [*Villareal*, 1999] and members of the genera *Rhizosolenia* [*Villareal et al.*, 1999], can migrate below the euphotic zone to acquire nitrate. An earlier attempt was made to assess whether vertical migration may also supply iron by measuring the ferridoxin/flavodoxin ratio in rising and sinking *Rhizosolenia sp.* mats [*McKay et al.*, 2000]. The results were inconclusive because no change in flavodoxin was seen, even with *Rhizosolenia* cells incubated in the presence of high iron concentrations. We examined the potential for vertical migration of large phytoplankton into high iron waters below the ferricline to supply iron during the Fe Vertical Transport (FEVER) cruise on the Research Vessel Western Flyer from October 17 to 28, 2005.

2. Methods

Dissolved iron (0.2 µm filter) was measured at sea in samples acidified to pH 3 and on shore in the same samples after acidification to pH 1.8 for one month using techniques

for sample collection and analysis that were described previously [*Johnson et al.*, 2003]. Samples for iron analysis were collected with a rosette sampler and 2.5 l, external closure bottles modified for trace metal sampling [*Johnson et al.*, 2003]. Chlorophyll was determined by filtering one liter of seawater onto Whatman GFF filters and extracting in cold acetone for one day before fluorometric analysis. Nitrate concentrations were determined in discrete samples using an Alpkem RFA automated analyzer and with in situ sensors [*Johnson and Coletti*, 2002].

The effects of vertical migration were studied by collecting phytoplankton in 7.6 liter polycarbonate sample containers with conical tops and bottoms that were deployed on the Remotely Operated Vehicle Tiburon (Auxiliary Material, Fig. 1). Assuming that phytoplankton vertical migration contributes significantly to chemical transport, then phytoplankton vertical velocities must be greater than several 10's of meters per day to translocate from the euphotic zone to depths near the ferricline and back in a reasonable time. At these velocities, the rising population of the captured cells should aggregate in the top cone of the sampler, while the sinking cells are likely to be found in the bottom cone within an hour. To allow for such separation, the samplers were held in a cold room at 14°C, near ambient temperature, for one hour following each ROV dive, in addition to one to two hours that had elapsed after sampler closure while the ROV was in the water. Two to ten paired samples (2 to 250 ml) were then withdrawn from the top and bottom cones by slowly displacing the distal volumes with 0.2 µm filtered surface seawater through a fitting at the middle of each sampler.

Variable fluorescence parameters [*Kolber et al.,* 1994; *Behrenfeld et al.,* 1996] were measured on samples from the top and bottom cones of the ROV sampler and from

hydrocast samples. Unfiltered samples were analyzed on all ROV dives. In addition, samples were size fractionated in some experiments with 5 µm filters (Poretics) on two ROV dives and 10 µm filters on three ROV dives. The benchtop fast repetition rate (FRR) fluorometer used to determine variable fluorescence was a new design with enhanced sensitivity. The variable fluorescence signal was readily detected at chlorophyll concentrations near 0.03 µg l^{-1}, typical of the 170 m samples. All FRR measurements were corrected for blank values using sampler water, sequentially filtered with Whatman GFF filters and then with Millipore 0.2 µm filters. Small amounts of iron contamination have negligible impact on variable fluorescence over the short time period from sample collection to analysis. The conical ROV samplers were acid cleaned and verified to have only low levels of iron contamination (typically <0.1 nM above ambient) by measuring samples from each depth on each ROV dive. Samples were also withdrawn from the ROV samplers for phytoplankton cell counts by epifluorescence microscopy.

3. Results and Discussion

The FEVER station was located 800 km (34°N, 129°W) off the California coast in highly oligotrophic waters. Estimated annual average primary production rates determined from satellite sensors at this location (508 mg C m^{-2} d^{-1} mean value from July 2002 to July 2005) are similar to Station ALOHA, the Hawaii Ocean Time series site (484 mg C m^{-2} d^{-1}) (data downloaded at http://oceanwatch.pfeg.noaa.gov/). The nitracline was found at depths ranging from 110 to 120 m. (Fig. 2a). The ferricline was found near 160 m (Fig. 2b), about 45 m below the nitracline.

The chlorophyll maximum is present at 90 to 100 m depth (Fig. 2c), well below the wind mixed layer, which extends to 45 m depth (Fig. 2d). The 1% light level, determined with a PAR sensor on the sampling rosette, occurred near 95 m depth (shown as a dashed line in Fig. 2c). The ferricline lies well below this light level or the community compensation irradiance value of 1.3 mol photons m^{-2} d^{-1} [*Siegel et al.*, 2002] at 70 m depth. Twenty percent of the extractable chlorophyll (Fig. 2c) and ten percent of the biomass estimated from the light attenuation signal in the upper 200 m (not shown) were found below the nitracline. The high chlorophyll to biomass ratio is indicative of a shade adapted phytoplankton community below the nitracline, rather than grazed and degraded material sinking to the bottom.

Samples were collected with the ROV at 100, 120, 140 and 170 m to assess phytoplankton vertical migration to acquire iron. These depths were selected to be above the nitracline, near the nitracline, near the ferricline and below the ferricline. The paired sets of samples from the top (rising cells) and bottom (sinking cells) cones of the ROV samplers were analyzed by Fast Repetition Rate (FRR) fluorometry. Open ocean iron fertilization experiments demonstrate unambiguously that variable fluorescence parameters of phytoplankton, which are detected by FRR, respond to iron acquisition [*Kolber et al.*, 1994; *Behrenfeld et al.*, 1996]. The mean photochemical quantum efficiency of photosynthesis (variable fluorescence F_v divided by maximal fluorescence F_m) in unfractionated samples collected during eleven ROV dives at 100 m, a depth above the ferricline and nitracline, was 0.58 for rising cells (Fig. 3a). This value is near the theoretical maximum value of 0.6 to 0.7 for photosynthesis, indicative of nutrient replete phytoplankton [*Kolber et al.*, 1994]. The cells from the bottom cone of the

samplers have significantly ($P<0.001$, t-test) lower F_v/F_m values (0.51), more indicative of iron stress. At greater depths, the difference in F_v/F_m becomes smaller and below the ferricline there was no difference between cells from the top and bottom cones (Fig. 3a).

The difference between quantum efficiency of photosynthesis in rising and sinking cells is indicative of vertical migration by photosynthetically-stressed cells to acquire iron. Vertical migration over distances of 10's of meters is generally thought to be possible only for large phytoplankton. Variable fluorescence in size-fractionated samples was measured to examine this mechanism further. The large (>5 or 10 µm) cells appear to be iron stressed with mean values of F_v/F_m (~0.46) that are significantly ($P<0.001$) lower than in the small cells at depths above 170 m (Fig. 3b). Small cells appear to be iron replete with F_v/F_m values near 0.6 at depths above 170 m. Similar patterns of iron stress were observed over the whole euphotic zone, with large cells generally displaying about 30% lower F_v/F_m than the small ones, which indicates the iron is not coming from above. This result is consistent with the "Ecumenical Hypothesis", which suggests that small cells can adapt more effectively to iron stress as they are more efficient at acquiring iron [*Morel et al.,* 1991].

The large, iron-limited cells must have an alternate strategy for iron acquisition. The capability of the large cells to migrate downward 10's of meters and acquire iron is demonstrated by comparing the F_v/F_m values in large cells collected from the top and bottom cones of the ROV sampler (Fig. 3c). The sinking cells at depths above the ferricline (100 and 120 m) have significantly ($P<0.05$ and $P<0.001$) lower F_v/F_m values than do the rising cells. There is no significant difference at or below the ferricline.

Large cells, which are rising above the ferricline, were more iron replete and must have acquired iron earlier in their transit.

Epifluorescence microscopy showed that the large cells are primarily the pennate diatoms *Fragilariopsis doliolus, Pseudonitzschia sp., Thallasiothrix sp.,* and *Thallasionema sp.* (in order of contribution to total cell carbon, which was estimated from cell size and published conversion factors for cell volume to carbon). The total number of large diatom cells per liter is small (order of 500 to 1000) and the diatoms contribute about 10% of the total cellular carbon, which is dominated by <5 µm cells. There are no statistically significant ($P>0.05$) differences in numbers of rising and sinking diatom cells (Fig. 4), indicating that there is an approximate balance in flux of cells through the water column.

The 40 m offset in the ferricline below the nitracline implies a substantial vertical migration would be required to obtain iron. Laboratory measurements of phytoplankton sinking rates seldom exceed a few meters per day, but iron deficiency clearly increases sinking rates in diatoms [*Muggli et al.,* 1996; *Waite and Nodder,* 2001]. Further, in situ observations of phytoplankton sinking rates can be very high, on the order of 100's of meters per day [*DiTullio et al.,* 2000]. Iron-limited diatoms in the ocean increase their $Si:NO_3$ uptake ratio, forming additional ballast [*Hutchins and Bruland,* 1998]. Sinking in iron-fertilized, experimental patches occurs very soon after the onset of iron limitation [*Boyd et al.,* 2005]. These observations suggest that rapid descent to the ferricline by iron-limited diatoms is feasible, but leaves open the question of how buoyancy is restored. Perhaps diatoms possess a capability for de-ballasting silica, which accounts for the large (~60%), but variable (10 to 100%), fraction of biogenic silica production that

dissolves near the base of the euphotic zone [*Rageneau et al.*, 2000]. This capability may be related to the ability of the enzyme carbonic anhydrase to use diatom silica as a proton donor [*Milligan and Morel*, 2002].

Recently, attention has been focused on nutrient stocks in thermocline waters of the low latitude ocean as a major control on primary production [*Sarmiento et al.*, 2004; *Palter et al.*, 2005]. Our results suggest an additional mechanism for control of ocean productivity by thermocline nutrients. If iron concentrations increased during glacial periods, then much of the nitrate that now lies above the ferricline in the Pacific would also become accessible during vertical migration. This presumes that vertical migration, which now transports some nitrate [*Villareal et al.*, 1999], would become more efficient when the low iron condition at the nitracline is relieved. Thick deposits of the vertical migrating diatom *E. rex*, which were present in net tows at the FEVER station, are found in deep-sea sediment cores during glacial periods [*Broecker et al.*, 2000]. These deposits demonstrate that vertical migration can become more efficient in glacial periods. Large diatoms from the nutricline region are responsible for much of the annual carbon export [*Kemp et al.*, 2000].

Acknowledgements. This work was supported by the David and Lucile Packard Foundation. Participation by R.A.F. was sponsored by the Gordon and Betty Moore Foundation. We thank the crew of the R/V Western Flyer and ROV Tiburon for their assistance.

References

Archer, D., A. Winguth, D. Lea, and N. Mahowald (2000), What caused the glacial/interglacial atmospheric PCO2 cycles? Rev. Geophys., 38, 159-189.

Behrenfeld, M. J., A. J. Bale, Z. S. Kolber, J. Aiken, and P. W. Falkowski (1996), Confirmation of iron limitation of phytoplankton photosynthesis in the equatorial Pacific Ocean. Nature, 383, 508 – 511.

Boyd, P. W., et al. (2005), The evolution and termination of an iron-induced mesoscale bloom in the northeast subarctic Pacific. Limnol. Oceanogr. 50, 1872-1886.

Boyle, E. A., B. A. Bergquist, and R. A. Kayser, (2005) Iron, manganese, and lead at Hawaii Ocean Time-series Station ALOHA: Temporal variability and an intermediate water hydrothermal plume, Geochim. Cosmochim. Acta 69, 933-952.

Broecker, W. S. et al. Late glacial diatom accumulation at 9°S in the Indian Ocean. Paleoceanogr. 15, 348-352 (2000).

Coale, K. H. et al. Southern Ocean Iron Enrichment Experiment: Carbon cycling in high- and low-Si waters. Science 304, 408-141 (2004).

Coale, K. H., Gordon, R. M. & Wang, X. J. The distribution and behavior of dissolved and particulate iron and zinc in the Ross Sea and Antarctic circumpolar current along 170° W. Deep-Sea Res. Part I 52, 295-318 (2005).

DiTullio, G. R. et al. Rapid and early export of Phaeocystis antarctica blooms in the Ross Sea, Antarctica. Nature 404, 595-598 (2000).

Duce, R. A. & Tindale, N. W. Atmospheric transport of iron and its depostion in the ocean. Limnol. Oceanogr. 36, 1715-1726 (1991).

Fung, I., Meyn, S., Tegen, I., Doney, S.C., John, J. & Bishop, J.K.B. Iron supply and demand in the upper ocean. Global Biogeochem. Cycles 14, 281-296 (2000).

Hutchins, D. A. & Bruland, K. W. Iron-limited diatom growth and Si:N uptake ratios in a coastal upwelling regime. Nature 393, 561 - 564 (1998).

Johnson, K. S. & Coletti, L. J. In situ ultraviolet spectrophotometry for high resolution and long term monitoring of nitrate, bromide and bisulfide in the ocean. Deep-Sea Res. I, 49, 1291-1305 (2002).

Johnson, K. S., et al. Surface ocean-lower atmosphere interactions in the Northeast Pacific Ocean gyre: Aerosols, iron and the ecosystem response. Global Biogeochemical Cycles 17, GB1063, doi:10.1029/2002GB002004 (2003).

Johnson, K. S., Gordon, R. M. & Coale, K. H. What controls dissolved iron in the world ocean? Mar. Chem. 57, 137-161 (1997a).

Johnson, K. S., Gordon, R. M. & Coale, K. H. What controls dissolved iron in the world ocean: Authors closing comments. Mar. Chem. 57, 181-186 (1997b).

Karl, D. M. A sea of change: Biogeochemical variability in the North Pacific subtropical gyre. Ecosystems 2, 181-214 (1999).

Kemp, A.E.S., Pike, J. Pearce, R.B. & Lange, C.B. The “fall dump”: a new perspective on the role of a shade flora in the annual cycle of diatom production and export flux. Deep-Sea Res. II, 47, 2129-2154 (2000).

Kolber, Z. S. et al. Iron limitation of phytoplankton photosynthesis in the equatorial Pacific Ocean. Nature 371, 145-149 (1994).

McKay, R. M. L., Villareal, T. A. & La Roche, J. Vertical migration by Rhizosolenia spp. (Bacillariophyceae): Implications for Fe acquisition. J. Phycol. 36, 669-674 (2000).

Milligan, A. J. and F. M. M. Morel (2002) A proton buffering role for silica in diatoms, Science, 297, 1848-1850.

Moore, J. K., S. C. Doney and K. Lindsay (2004), Upper ocean ecosystem dynamics and iron cycling in a global three-dimensional model, Global Biogeochem. Cycles, 18, GB4028, doi:10.1029/2004GB002220.

Morel, F. M. M., J. G. Reuter and N. M. Price (1991). Iron nutrition of phytoplankton and its possible importance in the ecology of ocean regions with high nutrient and low biomass, Oceanography, 4, 56−61.

Muggli, D. L., Lecourt, M. & Harrison, P. J. Effects of iron and nitrogen source on the sinking rate, physiology and metal composition of an oceanic diatom from the subarctic Pacific. Mar. Ecol. Prog. Ser. 132, 215-227 (1996).

Palter, J. B., Lozier, M. S. & Barber, R. T. The effect of advection on the nutrient reservoir in the North Atlantic subtropical gyre. Nature 437, 687-692 (2005).

Ragueneau, O., et al. A review of the Si cycle in the modern ocean: recent progress and missing gaps in the application of biogenic opal as a paleoproductivity proxy. Global Planet. Change 26 317-365 (2000).

Sarmiento, J. L., Gruber, N., Brzezinski, M. A. & Dunne, J. P. High-latitude controls of thermocline nutrients and low latitude biological productivity. Nature 427, 56-60 (2004).

Siegel, D. A., Doney, S. C. & Yoder, J. A. The North Atlantic spring phytoplankton bloom and Sverdrup's critical depth hypothesis. Science 296, 730-733 (2002).

Villareal, T. A. Biological and chemical characteristics of the giant diatom Ethmodiscus (bacillariophyceae) in the central North Pacific gyre. J. Phycol. 35, 896-902 (1999).

Villareal, T. A. et al. Upward transport of oceanic nitrate by migrating diatom mats. Nature 397, 423-425 (1999).

Waite, A. M. & Nodder, S. D. The effect of in situ iron addition on the sinking rates and export flux of Southern Ocean diatoms. Deep-Sea Res. II, 48, 2635-2654 (2001).

V. Elrod, S. Fitzwater, K. Johnson, D. Klimov, Z. Kolber, J. Needoba, Monterey Bay Aquarium Research Institute, 7700 Sandholdt Road, Moss Landing, CA 95039, USA. (johnson@mbari.org)

R. Foster, Ocean Sciences Department, University of California, Santa Cruz, CA 95064, USA.

S. Tanner, Moss Landing Marine Laboratories, 8272 Moss Landing Road, Moss Landing, CA 95039, USA.

johnson@mbari.org

Figure Legends

Figure 1. Vertical profiles of dissolved iron (●) and nitrate (○). Horizontal arrows show locations of the ferricline (solid line) and nitracline (dashed line). a Iron, nitrate in the Northeast Pacific (34°N, 128.5°W; *Johnson et al.,* 2003). b Iron, nitrate in the tropical North Pacific (15°N, 140°W; *Johnson et al.,* 1997a). c Iron, nitrate in the tropical South Pacific (12°S, 145°W; *Johnson et al.,* 1997a). d Iron, nitrate in the Pacific sector of the Southern Ocean (61°S, 170°W; *Coale et al.,* 2005). Southern Ocean samples are from January, while the diamonds in panel d are nitrate for November and show the depth extent over which nitrate is drawn down in the Southern Ocean summer bloom, relative to the depth of the ferricline.

Figure 2. Vertical profiles of chemical, physical and biological properties at the FEVER Station (34ºN, 129ºW). a, Nitrate determined with an In Situ Ultraviolet Spectrophotometer (solid line) and in discrete samples collected in Niskin bottles (solid circles). b, Dissolved (0.2 µm filter) iron concentrations determined on board ship in samples at pH 3 (open squares) and after one month at pH 1.8 (solid circles). Each symbol represents the mean value from three different vertical profiles collected on separate days. Error bars are the 90% confidence limits for the mean. c, Chlorophyll concentration in filtered (GFF) samples determined by extraction in cold acetone (solid circles). The chlorophyll fluorescence signal from an in situ fluorometer (solid line) was scaled to fit the extracted values. Dashed horizontal line is the 1% light level. d, Temperature determined in situ.

Figure 3. Photochemical quantum efficiency of photosynthesis (F_v/F_m) versus depth in samples collected by ROV. a, Unfiltered samples collected from the top (Δ) and bottom (∇) cones of the ROV sampler. Symbols indicate the presumed direction that the phytoplankton were migrating. b, Mean values for samples from size fractionation experiments: large fraction (◊) and small fraction (o). c, Mean values for the large size fraction collected from the top (Δ) and bottom (∇) cones of the ROV sampler. All error bars are 95% confidence limits for the mean. ** indicates differences in mean values with $P<0.01$, * indicates difference with $P<0.05$.

Figure 4. Abundance of large (>5 µm) diatom cells in the top (Δ) and bottom (∇) cones of the ROV sampler. Error bars are 90% confidence intervals.

Figure 1

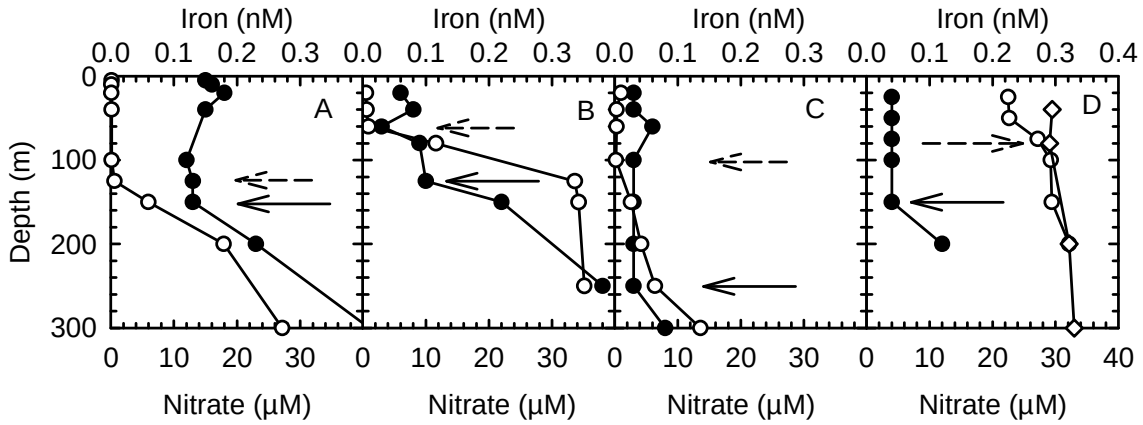
Iron (nM)
0.0 0.1 0.2 0.3
Iron (nM)
0.0 0.1 0.2 0.3
Iron (nM)
0.0 0.1 0.2 0.3
Iron (nM)
0.0 0.1 0.2 0.3 0.4
A
B
C
D
Depth (m)
0
100
200
300
0 10 20 30
0 10 20 30
0 10 20 30
0 10 20 30 40
Nitrate (µM)
Nitrate (µM)
Nitrate (µM)
Nitrate (µM)

Figure 2

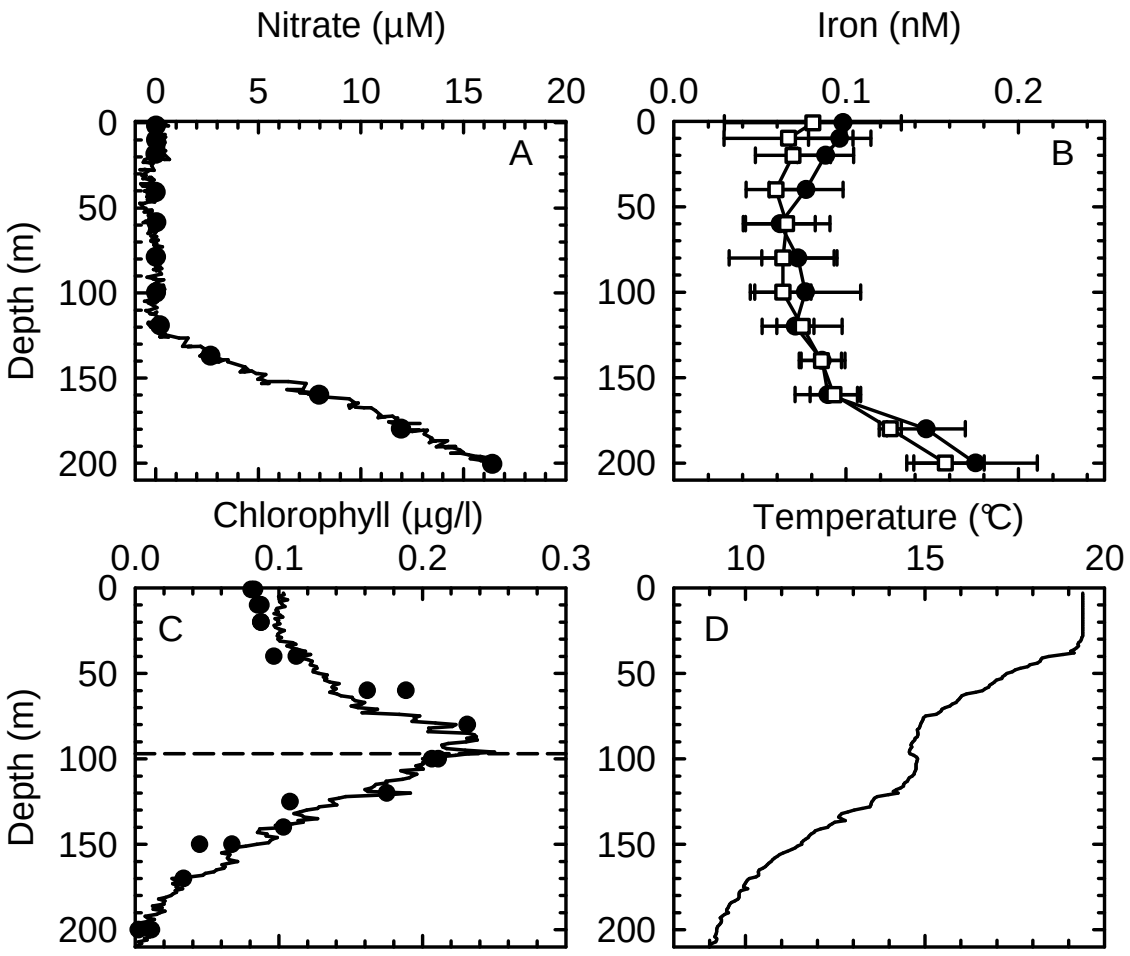
Nitrate (µM)
0
5
10
15
20
Iron (nM)
0.0
0.1
0.2
A
B
Depth (m)
0
50
100
150
200
Chlorophyll (µg/l)
0.0
0.1
0.2
0.3
Temperature (℃)
10
15
20
C
D

Figure 3

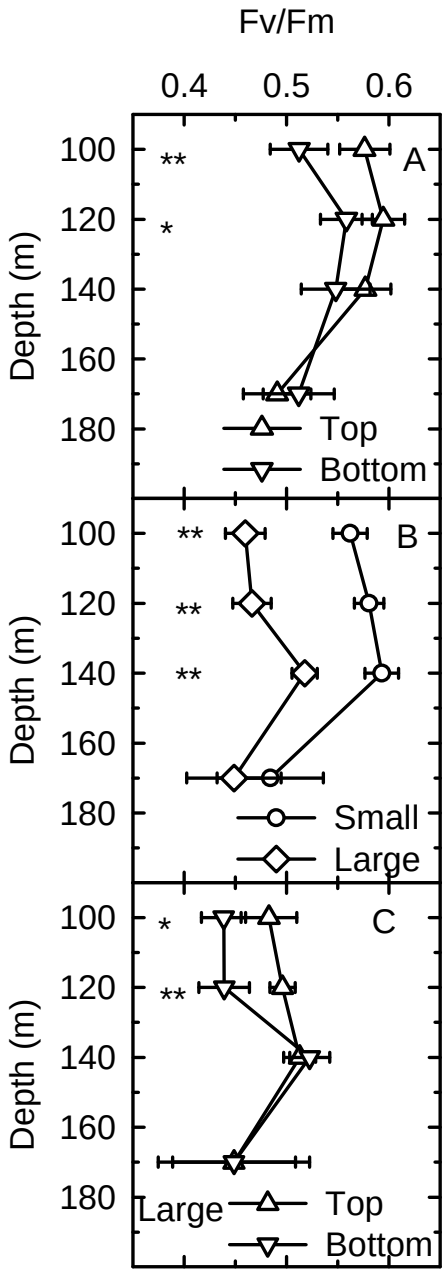
Fv/Fm
0.4
0.5
0.6
Depth (m)
100
120
140
160
180
**
*
A
Top
Bottom
**
**
**
B
Small
Large
*
**
C
Large
Top
Bottom

Figure 4

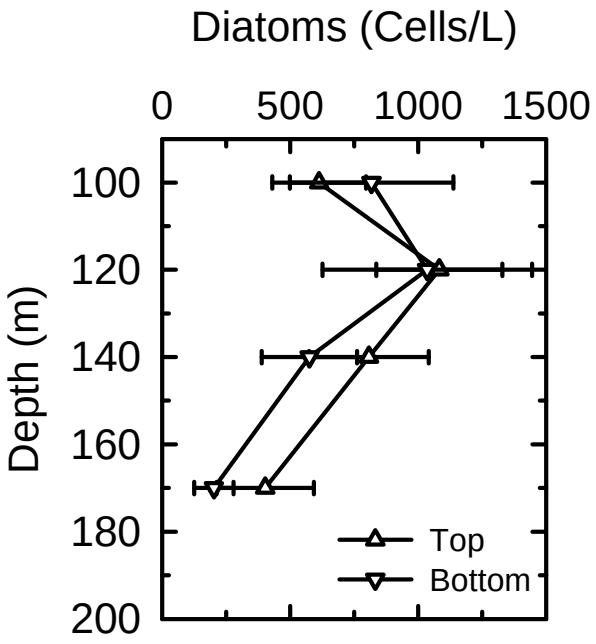
Diatoms (Cells/L)
0
500
1000
1500
Depth (m)
100
120
140
160
180
200
Top
Bottom

Auxiliary Material, Figure 1

ROV actuated sampler used to separate rising and sinking cells shown in the closed and open positions. The sampler is constructed from polycarbonate and has an internal diameter of 16.3 cm. The middle section is 30.5 cm long and the cones are 9.2 cm in height. The samplers are closed using hydraulic actuators on the ROV Tiburon.